Ecological Applications, 18(7), 2008, pp. 1781–1794

USING DEMOGRAPHY AND MOVEMENT BEHAVIOR TO PREDICT RANGE EXPANSION OF THE SOUTHERN SEA OTTER

M. Tim Tinker,[1,4] Daniel F. Doak,[2] and James A. Estes[3]

[1]*U.S. Geological Survey, Western Ecological Research Center, Long Marine Laboratory, 100 Shaffer Road, Santa Cruz, California 95060 USA*
[2]*Department of Zoology and Physiology, University of Wyoming, 1000 E. University Avenue, Department 3166, Laramie, Wyoming 82071 USA*
[3]*Department of Ecology and Evolutionary Biology, University of California, Center for Ocean Health, 100 Shaffer Road, Santa Cruz, California 95060 USA*

Abstract. In addition to forecasting population growth, basic demographic data combined with movement data provide a means for predicting rates of range expansion. Quantitative models of range expansion have rarely been applied to large vertebrates, although such tools could be useful for restoration and management of many threatened but recovering populations. Using the southern sea otter (*Enhydra lutris nereis*) as a case study, we utilized integro-difference equations in combination with a stage-structured projection matrix that incorporated spatial variation in dispersal and demography to make forecasts of population recovery and range recolonization. In addition to these basic predictions, we emphasize how to make these modeling predictions useful in a management context through the inclusion of parameter uncertainty and sensitivity analysis. Our models resulted in hind-cast (1989–2003) predictions of net population growth and range expansion that closely matched observed patterns. We next made projections of future range expansion and population growth, incorporating uncertainty in all model parameters, and explored the sensitivity of model predictions to variation in spatially explicit survival and dispersal rates. The predicted rate of southward range expansion (median = 5.2 km/yr) was sensitive to both dispersal and survival rates; elasticity analysis indicated that changes in adult survival would have the greatest potential effect on the rate of range expansion, while perturbation analysis showed that variation in subadult dispersal contributed most to variance in model predictions. Variation in survival and dispersal of females at the south end of the range contributed most of the variance in predicted southward range expansion. Our approach provides guidance for the acquisition of further data and a means of forecasting the consequence of specific management actions. Similar methods could aid in the management of other recovering populations.

Key words: asymptotic wave speed; Enhydra lutris nereis; *integro-difference equations; life stage simulation analysis; multistate projection matrix; range expansion; southern sea otter.*

Introduction

Data on stage-specific probabilities of survival, growth, and reproduction have long been used by ecologists to understand past and present population dynamics (e.g., Caswell 2001, Morris and Doak 2002) and can also be used for predicting future trends. This is especially important in the case of threatened or endangered species, since effective management strategies for these populations require reliable information about the life-history stages with the greatest potential for enhancing or limiting recovery (Crouse et al. 1987, Beissinger and McCullough 2002). Many rare species have been reduced to small, fragmented populations and extirpated from much of their historical range, so that recovery depends not only on enhanced population size but also on recolonization of the species' former range (Swenson 1999, Moro 2003). In addition to forecasting population growth, basic demographic and movement data provide a means for predicting rates of range expansion, using analytical tools that have been available for many years (Skellam 1951, Andow et al. 1990). For example, the study of invasive species has begun to benefit from the use of reaction–diffusion models (Shigesada et al. 1995) and integro-difference equations (Kot et al. 1996), which often provide robust predictions of invasion speed (Neubert and Parker 2004). These methods have only rarely been applied to large vertebrates (e.g., Lubina and Levin 1988, Lensink 1997, Hurford et al. 2006), but with the increasing number of threatened vertebrate populations that are reinhabiting former ranges and improving technologies to determine large-scale movement behaviors, these tools may have considerable potential value for conservation management. Here, we adapt this modeling framework to address management predictions and key concerns for a recovering carnivore population, the southern sea otter (*Enhydra lutris nereis*).

Manuscript received 3 May 2007; revised 21 January 2008; accepted 17 March 2008. Corrresponding Editor: S. S. Heppell.
[4] E-mail: tinker@biology.ucsc.edu

Prior to the North Pacific fur trade of the 18th and 19th centuries, sea otters were important apex predators in nearshore coastal marine communities ranging from northern Japan to Baja California, but they were hunted to the edge of extinction by the early 1900s (Kenyon 1969). Once protected by international treaty, sea otter populations recovered over much of their former range. In California, however, the southern subspecies remains listed as threatened by the Endangered Species Act (USFWS 2003). Full recovery of this population has for decades been limited by slow population growth; at least in recent years, this problem has been largely due to elevated mortality among prime-age females (Estes et al. 2003, Gerber et al. 2004, Tinker et al. 2006). Management agencies are particularly interested in the development of a realistic predictive model of population recovery and range expansion into southern California, as this will facilitate the informed assessment of potential impacts of sea otters on important industries (e.g., fisheries, eco-tourism), potential negative effects of human activity on sea otters (e.g., risks associated with the nearshore transport and extraction of petroleum, entanglement in fishing gear, etc.), and eventual delisting of this subspecies (USFWS 2003). The existence of spatially explicit demographic and movement information for the southern sea otter over the whole of its range (Tinker et al. 2006) makes this an ideal species for developing a predictive model of population growth and range expansion for a large carnivore and for exploring the sensitivity of the model predictions to parameter estimates over multiple spatial scales.

Two prior analyses of range expansion of this population have shown the promise of demographic-movement models to successfully capture its spatial dynamics (Lubina and Levin 1988, Krkošek et al. 2007). Like many published uses of movement models, these studies focus on technical aspects of model development and validation, rather than on data quality issues or the problems inherent in making this approach directly applicable to the key concerns of conservation managers. As with management of many rare species, the management concerns about range expansion of sea otters largely involve short-term, regional predictions of distribution and population growth and also the need to directly confront uncertainty in predictions due to limited data.

In response to these needs, our goal here is to show how the marriage of two well-tested analytical techniques, population projection matrices structured by stage and region and integro-difference equations, can be adapted to make useful predictions for the management of a recovering population. To do so, we account for uncertainty in all model parameters using Monte Carlo simulations, and we use sensitivity analysis to explore and contrast the relative importance of dispersal and vital rate parameters in different portions of the range for model predictions, thereby highlighting areas in which further study will be particularly useful. We focus our analysis on southward range expansion of California sea otters, both for simplicity and because this region is of particular concern for management agencies (USFWS 2005). In this work we seek to strike a balance between relevance for applied conservation and general applicability of results: the approach we use, while obviously tailored specifically for southern sea otters, is also designed to be useful in addressing the dynamics of other recovering species.

Making careful predictions of range expansion and exploring the factors controlling these dynamics is of broad relevance in conservation. Large carnivores and mega-herbivores (especially mammals) are or once were components of most natural ecosystems, but these species have been among the first to disappear with the erosion of biodiversity (Ray et al. 2005). There is also growing evidence that many large carnivores act as keystone species (sensu Paine 1966, 1969, Power et al. 1996), exerting strong and sometimes far-reaching effects on ecosystem structure and function through top-down processes (e.g., Estes et al. 1998, Pace et al. 1999, Berger et al. 2001, Terborgh et al. 2001). For these reasons, and because these species typically require larger areas than most other species for the maintenance of viable populations, their reestablishment is viewed as an important ingredient in developing conservation strategies and restoring degraded ecosystems (Soulé et al. 2003, Ripple and Beschta 2007). As a result of focused conservation efforts, multiple large mammals are now recovering or have the potential to recover and re-expand into at least parts of their ranges (Comiskey et al. 2002, Lindsey et al. 2004, Bales et al. 2005, Kojola and Heikkinen 2006, Kojola et al. 2006, Neflemann et al. 2007), creating the need to better anticipate rates and patterns of range expansion and to determine how best to manage this population growth.

Model Development

Overview of model structure

Previous analyses suggested that spatial variation in sea otter vital rates could best be represented by dividing the California sea otter range into three contiguous regions (corresponding to the northern, central, and southern portions of the range) among which there were substantial differences in annual survival (Tinker et al. 2006). To facilitate the tracking of simulation results at the range boundaries, we defined two additional regions that corresponded to the expanding frontal zones at the north and south ends of the current range of sea otters in California (Fig. 1): in so doing we assume that demographic rates and dispersal patterns for otters in the southern frontal zone were identical to those in the adjacent southern region, while the otters in the northern frontal zone were governed by the rates estimated for the adjacent northern region.

For each of the five regions we modeled demographic processes using a stage-based projection matrix to describe annual transitions between four age classes:

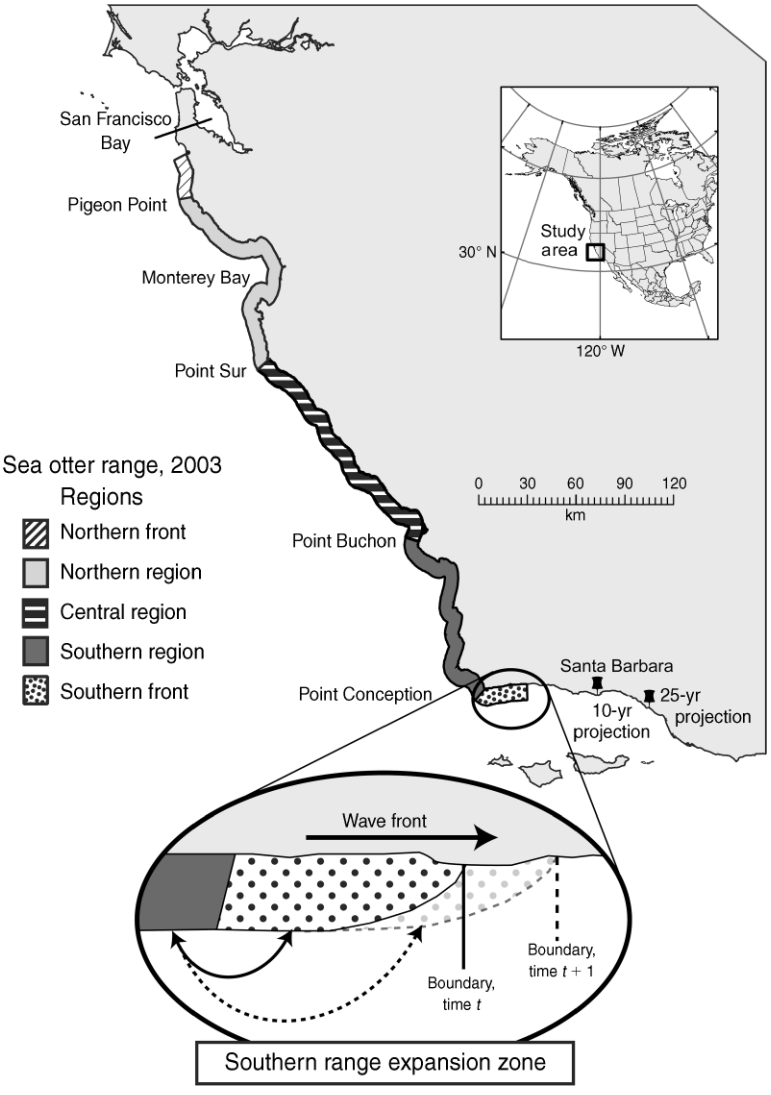

FIG. 1. Map of central California, USA, showing current range of the southern sea otter (*Enhydra lutris nereis*; excluding San Nicolas Island) and identifying the spatial arrangement of the five regions used for the simulation model. The dynamics of range expansion (as modeled using integro-difference equations) are illustrated in a blow-up of the southern frontal zone. The point estimates for the 10-year and 25-year projections of the location of the southern range end boundary are also shown, based on the results of the simulation model (see Table 4).

juveniles (defined as one year post-weaning), subadults (two- and three-year-olds), prime-age adults (4–10-year-olds), and aged adults (11 years of age or older). We used a stage-structured matrix (rather than age-structured) to simplify interpretation of results and for consistency with available data sets. Transitions were tracked separately for females and males, resulting in a two-sex 8×8 demographic matrix, **A**, for each region (Table 1). Three types of transition were identified: G represents survival and growth, or the probability of individuals surviving for one year and advancing to the next age class; P represents "persistence," or survival without transition to the next age class; and R represents survival and successful reproduction (for our purposes, an individual female is considered to have successfully reproduced if she gives birth and successfully weans a pup; i.e., she contributes a single viable juvenile to the population). To estimate P, G, and R we used standard equations for deriving fixed-stage-duration transition probabilities from underlying vital rates (Caswell 2001):

$$P_{j,i} = s_i \times \left[1 - \frac{(s_i/\lambda)^{T_i} - (s_i/\lambda)^{T_i-1}}{(s_i/\lambda)^{T_i} - 1}\right] \quad (1)$$

$$G_{j,i} = s_i \times \left[\frac{(s_i/\lambda)^{T_i} - (s_i/\lambda)^{T_i-1}}{(s_i/\lambda)^{T_i} - 1}\right] \quad (2)$$

$$R_{j,i} = s_i \times 1/2b_i \times w_i \quad (3)$$

TABLE 1. Representation of the demographic matrix **A** used to project annual demographic transitions for southern sea otters (*Enhydra lutris nereis*) in California, USA.

Age	j = stage at time $t+1$	i = stage at time t							
		1	2	3	4	5	6	7	8
Female									
Juvenile	1	0	$R_{1,2}$	$R_{1,3}$	$R_{1,4}$	0	0	0	0
Subadult	2	$G_{2,1}$	$P_{2,2}$	0	0	0	0	0	0
Adult	3	0	$G_{3,2}$	$P_{3,3}$	0	0	0	0	0
Aged adult	4	0	0	$G_{4,3}$	$P_{4,4}$	0	0	0	0
Male									
Juvenile	5	0	$R_{5,2}$	$R_{5,3}$	$R_{5,4}$	0	0	0	0
Subadult	6	0	0	0	0	$G_{6,5}$	$P_{6,6}$	0	0
Adult	7	0	0	0	0	0	$G_{7,6}$	$P_{7,7}$	0
Aged adult	8	0	0	0	0	0	0	$G_{8,7}$	$P_{8,8}$

Notes: Transitions are shown for eight stages, with 1–4 corresponding to female age classes and 5–8 corresponding to male age classes. Following standard convention, matrix elements represent transitions made from stage i (as indicated in the column headers) to stage j (as indicated in the rows of the second column) between year t and year $t+1$. The three possible transitions are G (survival and growth to the next age class), P (survival without transition to the next age class), and R (survival and successful reproduction).

where T_i is the stage duration (in years) for age/sex class i, λ is the annual rate of population growth, s_i is the annual survival rate for an individual of stage i, b_i represents the birth rate (assuming a 1:1 sex ratio at birth), and w_i is the weaning success rate for a female of stage i. Eqs. 1 and 2 were solved initially with $\lambda = 1$ and then updated with the new value of λ (derived algebraically from the resulting matrix) and resolved until the value of λ stabilized (Caswell 2001). Eqs. 1–2 assume that vital rates are constant, there is a stable age distribution, and there is no explicit density dependence. While the first two of these assumptions were violated to some degree, as explained below, Monte Carlo simulations indicated that the approximations provided sufficiently accurate results within the projection period and range of λ values evaluated. Specifically, at the end of a 25-year projection period we found negligible differences between age-structured matrices and their stage-structured equivalents with respect to final age composition and abundance estimates.

In addition to describing vital rates within each of the five regions, our model also had to account for dispersal of individuals between regions. Accordingly, dispersal rates for each age/sex class (calculated as explained below) were incorporated into a movement matrix, **M**, whose nonzero diagonal elements consisted of the estimated annual probabilities of moving to region y from region x for an otter of stage i ($m^i_{y,x}$). The **M** and **A** matrices were then combined, using methods described in detail by Hunter and Caswell (2005), in order to project changes to the population vector, a 40×1 array giving the number of animals in age/sex class i within region x at time t. For computational simplicity we assumed that individuals disperse at the start of each year, after which survival, growth, and reproduction occur according to the vital rates associated with the new location (Hunter and Caswell 2005). This approach of combining separate movement and demography matrices simplifies bookkeeping for our multisite models, but results in the same final structure as that used by other studies of combined demography and dispersal processes (Wootton and Bell 1992, Kauffman et al. 2004, Gerber et al. 2005).

Calculating dispersal rates

To calculate dispersal probabilities, we first noted that variation in annual net linear displacement (sensu Turchin 1998) of sea otters in California was well described by a Laplace distribution with parameter $\sigma_{i,x}$ (Fig. 2). The parameter $\sigma_{i,x}$ represents the expected net annual dispersal distance by an otter of stage i located at x' (where x' is defined as a point on the coast somewhere within subpopulation x). Note that for our current purposes we use the term "dispersal" to describe the average probability of an individual moving from x' to y' between time t and time $t+1$; this definition makes no reference to the biological cause or behavioral significance of such movements, which likely differ between age and sex classes. The Laplace distribution, which consists of two back-to-back exponential distributions, is convenient for modeling sea otter movements in California because animals are restricted to essentially one-dimensional movement north or south along the coastline (Lubina and Levin 1988, Krkošek et al. 2007). Other probability distributions can also be used to model long-distance movements, including so-called "fat-tailed" or leptokurtic dispersal kernels (Krkošek et al. 2007). Like Krkošek and co-authors, we found that fat-tailed kernels provided a marginally better fit to most of our dispersal data, especially those for juvenile males, but that use of these distributions led to an inadequate description of medium- to long-term population range expansion, as we describe in the following section.

The annual probability that an otter of stage i located at point x' disperses into region y ($m^i_{y,x'}$) was calculated as the absolute difference between Laplace cumulative

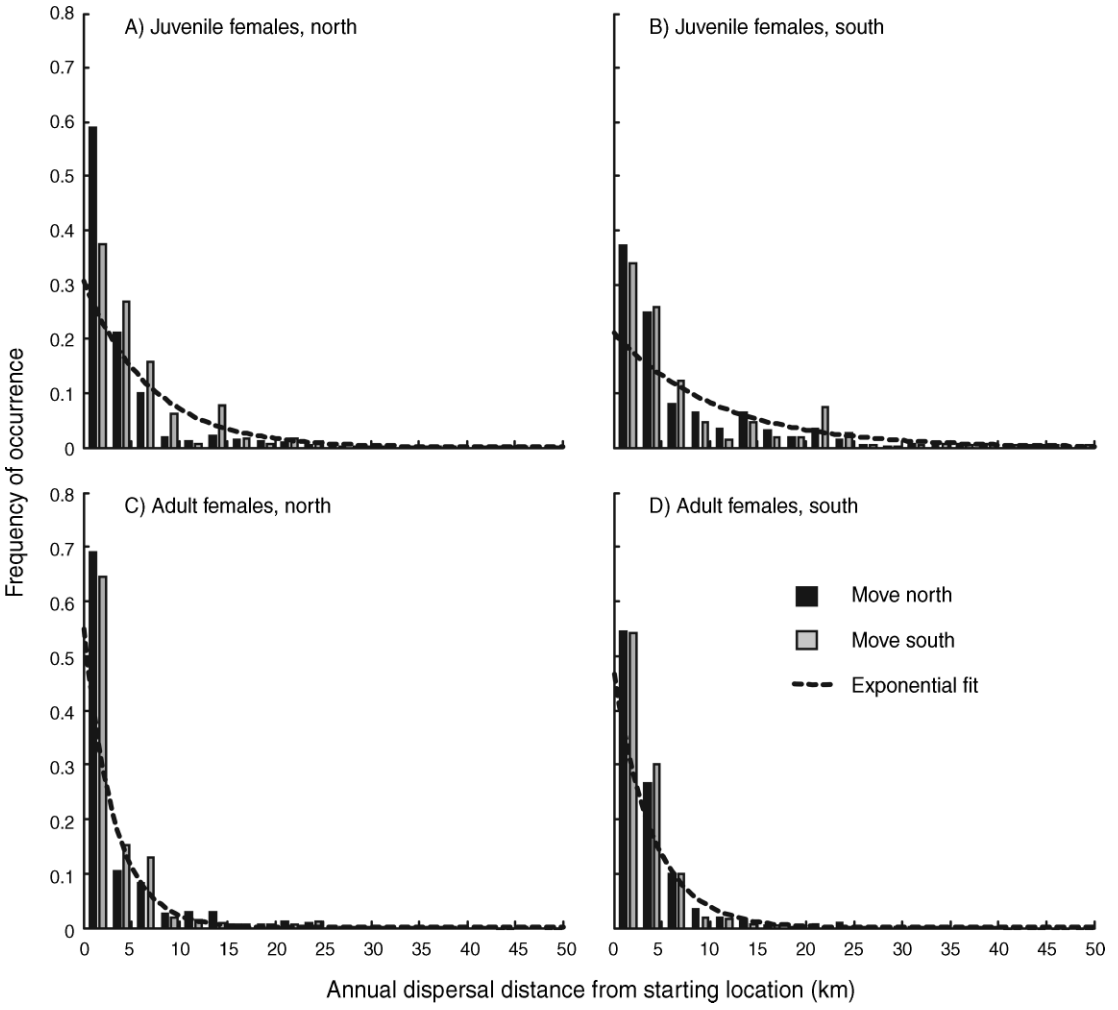

FIG. 2. Annual dispersal distance frequency histograms for juvenile/subadult females (top panels) and adult females (bottom panels) in the northern half of the range (left panels) and in the southern half of the range (right panels). Black bars show northward movements, and gray bars show southward movements. The corresponding Laplace density functions (dashed lines) are superimposed over the histograms. Note that the distributions for juvenile females show greater dispersion than those of adults, with the greatest dispersion in the southern portion of the range, a tendency that is reflected by a higher value of the Laplace distribution scale parameter, σ (see Table 3).

density functions evaluated at $|y_N - x'|$ and $|y_S - x'|$, where y_N and y_S are the northern-most and southern-most points along the coast in region y. We specified all locations and distances in terms of 500-m units along the one-dimensional axis described by the 10-m bathymetric contour, increasing from north to south (with "0" defined as the southern tip of the Golden Gate Bridge at the entrance to San Francisco Bay); we refer to this scale hereafter as the "as-the-otter-swims" or ATOS line (Pattison et al. 1997). We assumed that, for the purpose of measuring annual movement distances, all points within a 500-m interval (one ATOS unit) would be adequately represented by an integer value of x', so that the total probability of dispersal from region x to region y can be approximated as follows:

$$m^i_{y,x} = \sum_{x'=x_N}^{x_S} (m^i_{y,x'})p(x') \quad (4)$$

where $p(x')$ represents the probability that an individual from region x would be located at x' and thus must sum to 1 for $x_N \leq x' \leq x_S$. Based on the most recent 10 years of annual rangewide sea otter census data (which includes the ATOS location of each otter counted; data *available online*),[5] we calculated $p(x')$ as the cumulative number of otters observed at x' divided by the total number of otters observed anywhere between x_N and x_S. We solved Eq. 4 for each pair of regions, including cases of $y = x$ (the probability of remaining within the same region).

[5] ⟨http://www.werc.usgs.gov/otters/ca-surveys.html⟩

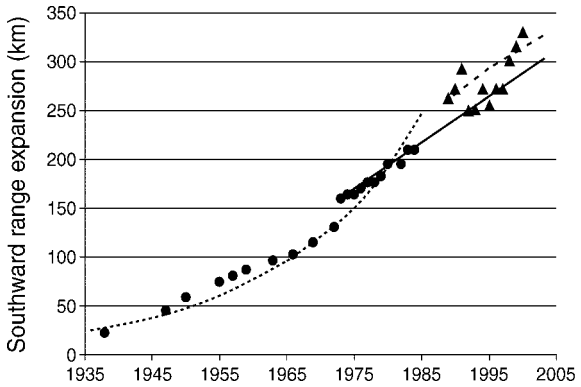

FIG. 3. Historical pattern of southward range expansion for sea otters in central California, from 1935 through 2005. The vertical axis shows the distance south of the initial population hub (Bixby Creek, in Big Sur) at which the southern range boundary was located at various points in time. Points prior to 1985 (circles) represent the "best-guess" locations, based on various survey techniques and anecdotal reports of sea otter sightings, while post-1985 data (triangles) represent standardized survey data (see footnote 5). Three hind-cast predictions of expected range expansion are shown, based on alternate methodological approaches: a linear rate of invasion predicted by a simple diffusion model (solid line; Lubina and Levin [1988]), an accelerating rate of invasion predicted by solving integro-difference equations with a fat-tailed dispersal kernel (dotted line; Krkošek et al. [2007]), and a linear rate of invasion predicted by solving integro-difference equations with an exponential dispersal kernel (dashed line; current analysis).

Range expansion

The multistate matrix model described in *Overview of model structure* accounts for movement and demographic processes within the existing range of the southern sea otter at time t. It does not, however, account for the continued expansion of the existing range boundaries to the north and south. In order to predict the rate of expansion of the population into unoccupied habitat, we used a stage-structured integro-difference equation model (following Neubert and Caswell 2000) to solve for the minimum asymptotic speed of the "traveling wave" formed by the population front (Fig. 1). The so-called "linear conjecture" hypothesizes that asymptotic wave speed will provide a reasonable prediction of population invasion speed so long as various assumptions are met (Weinberger 1982, Kot et al. 1996, Neubert and Parker 2004), including spatial and temporal environmental homogeneity (but see Neubert et al. 2000, Weinberger 2002) and lack of Allee effects or long-distance density dependence (Weinberger 1982). It has been found that Allee effects can result in invasion speeds that are slower than predicted (Hurford et al. 2006), but such effects seem unlikely for sea otters because individuals are not reliant on any sort of social group structure, and historical data indicate that sea otter populations have often increased rapidly from small initial population sizes (Jameson et al. 1982, Estes 1990). Moreover, a previous analysis of historical sea otter range expansion (Krkošek et al. 2007) has demonstrated reasonable agreement between observed invasion speed and that predicted by integro-difference equations. In that analysis, Krkošek et al. (2007) found that a variety of dispersal kernels were successful at predicting rates of range expansion, and although there was no obvious "best choice" they concluded that the accelerating invasion speeds predicted by fat-tailed kernels seemed most appropriate for explaining range expansion prior to 1980. With the addition of over 20 years of data (and a recognition of the dubious nature of many of the early 20th century data points used in past analyses) we, in contrast, found that a linear invasion speed is more consistent with the observed pattern of range expansion and especially so with the standardized survey data available from 1982 through the present (Fig. 3). For this reason, and because of the good fit between Laplace distributions and our telemetry-based dispersal data (Fig. 2), we formulated integro-difference equations using exponential dispersal kernels.

To predict southward range expansion, we used the demographic matrix **A** (Table 1) for the southern region and a dispersal moment-generating function matrix $\mathbf{D}(\omega)$, where ω is the parameter that determines the "shape" of the traveling wave at the population front. The matrix $\mathbf{D}(\omega)$ has the same dimensions as **A**, but its elements, $d_{j,i}(\omega)$, all equal 1 except for those on the diagonal and subdiagonal, which were set equal to the moment-generating functions of stage-specific exponential dispersal kernels evaluated at ω:

$$d_{j,i}(\omega) = \frac{1}{1 - \sigma_i^2 \omega^2} \tag{5}$$

where σ_i is the Laplace parameter for an animal of age/sex class i located in the southern portion of the range (Neubert and Caswell 2000). Element-by-element multiplication of the demographic matrix and moment-generating function matrix $[\mathbf{A} \circ \mathbf{D}(\omega)]$ produced a new matrix, $\mathbf{H}(\omega)$, from which we first calculated the maximum eigenvalue, $\rho_1(\omega)$, and then estimated the asymptotic wave speed (c):

$$c = \frac{1}{\omega^*} \ln \rho_1(\omega^*) \tag{6}$$

where ω^* is defined as the value of ω that minimizes "c" in Eq. 6. We used a similar approach to predict northward range expansion, substituting vital rates and dispersal kernels corresponding to the northern region. By using regionally specific parameter estimates for predicting asymptotic wave speed to the north and south, we allowed for differing rates of range expansion at either end of the range, consistent with historically observed patterns for this population (Lubina and Levin 1988, Riedman and Estes 1990). In so doing we assumed that animals from the range center do not directly contribute to range expansion or, more precisely, that they must first disperse to the northern or southern regions; this seems a reasonable assumption based upon

TABLE 2. Age- and sex-specific annual survival estimates used for the simulation model.

	Females				Males			
Study period	Juvenile	Subadult	Adult	Aged adult	Juvenile	Subadult	Adult	Aged adult
North								
1984–1986	0.85 (0.117)	0.88 (0.117)	0.93 (0.088)	0.65 (0.145)	0.88 (0.173)	0.86 (0.173)	0.7 (0.167)	0.50 (0.179)
1992–1994	0.86 (0.008)	0.86 (0.005)	0.89 (0.006)	0.76 (0.032)	0.77 (0.026)	0.77 (0.015)	0.79 (0.012)	0.62 (0.056)
1995–2001	0.83 (0.015)	0.83 (0.008)	0.86 (0.007)	0.71 (0.040)	0.73 (0.033)	0.72 (0.017)	0.75 (0.018)	0.56 (0.049)
Central								
1984–1986	0.85 (0.117)	0.88 (0.117)	0.93 (0.088)	0.65 (0.145)	0.88 (0.173)	0.86 (0.173)	0.70 (0.167)	0.50 (0.179)
1992–1994	0.89 (0.008)	0.89 (0.004)	0.89 (0.005)	0.71 (0.028)	0.82 (0.025)	0.81 (0.014)	0.80 (0.014)	0.56 (0.044)
1995–2001	0.87 (0.014)	0.86 (0.008)	0.86 (0.006)	0.67 (0.032)	0.78 (0.023)	0.77 (0.013)	0.75 (0.018)	0.51 (0.036)
South								
1984–1986	0.85 (0.117)	0.88 (0.117)	0.93 (0.088)	0.65 (0.145)	0.88 (0.173)	0.86 (0.173)	0.70 (0.167)	0.50 (0.179)
1992–1994	0.91 (0.019)	0.90 (0.012)	0.90 (0.010)	0.74 (0.032)	0.84 (0.028)	0.84 (0.020)	0.82 (0.017)	0.59 (0.050)
1995–2001	0.88 (0.017)	0.88 (0.013)	0.88 (0.011)	0.69 (0.038)	0.81 (0.021)	0.80 (0.016)	0.78 (0.021)	0.54 (0.043)

Notes: Values are reported as means with SE in parentheses. Estimates for 1984–1986 are based on values reported by Siniff and Ralls (1991). All other estimates are taken from Tinker et al. (2006).

typical annual dispersal distances measured from radio-tagged animals (Table 3).

We incorporated the resulting predictions of the rate of range expansion into projections of population growth by annually incrementing outward the areas encompassed by the two frontal zones: only the outer boundaries of the two frontal zones were adjusted, while all other boundary locations were held fixed. Each year's range expansion therefore impacted the following year's population dynamics through its effect on the solution to Eq. 4. The distribution of otters within each frontal zone was also recalculated each year: specifically, adjustments were made such that the relative abundance of animals at incremental distances in from the frontal boundary (the "shape" of the traveling wave) was held constant (Fig. 1).

MODEL PARAMETERIZATION

To account for the effects of parameter uncertainty on predictions of future population dynamics and sensitivity estimates, we used multiple estimates of demographic rates that spanned the range of historically observed population dynamics in California (Gerber et al. 2004). The first set of age- and sex-specific survival rate estimates used were taken from the mid-1980s (Siniff and Ralls 1991), a period when the population was growing at approximately 5% per year (the maximum historical rate of population growth for mainland California). Two additional sets of maximum-likelihood survival estimates were used (taken from Tinker et al. 2006): one corresponding to a period of slow population growth (1992–1994) and one to a period of slow population decline (1995–2001). The estimates from the 1980s did not account for spatial structure, while the latter two sets of estimates varied between the three main regions (Table 2). In contrast with the considerable variation in survival reported for sea otters, accumulating evidence suggests that there has been very little spatial or temporal variation in reproduction parameters over the past 20 years (Estes et al. 2003, Tinker et al. 2006); accordingly, we used a single set of age-specific reproductive rates for all simulations. Following Tinker et al. (2006), the age of first reproduction in females was assumed to occur at three years, the annual birth rate was set to 0.98 for all age classes, and age-specific weaning success rate was set to 0.37 for subadults, 0.58 for prime-age adults, and 0.72 for aged adults.

For each of the three sets of vital rate estimates (Table 2) we used the estimated means and standard errors to create sampling distributions with which to generate random sets of vital rates (following Gerber et al. 2004, Buckley et al. 2005). In order to create biologically realistic random survival schedules that maintained appropriate life-history-based correlations (i.e., recognizing that survival rates among age classes tend to covary), we first back-transformed each set of male and female stage-specific survival estimates into a logit function governing age effects on the annual rate of survival, s:

$$s_z = \frac{\exp[\theta_1 + \theta_2(z) + \theta_2(z^2)]}{1 + \exp[\theta_1 + \theta_2(z) + \theta_2(z^2)]} \quad (7)$$

where z is the median otter age (in years) for each stage. Maximum-likelihood techniques were used to find best-fit estimates of the three logit parameters (θ_1, θ_2, and θ_3) and the associated variance–covariance matrix. Assuming approximately normally distributed parameters in the logit function, we generated many random sets of logit parameter values such that the estimated means and variances/covariances were maintained (Morris and Doak 2002), and these were used to create random but "plausible" stage-specific survival rates.

Movement probabilities were estimated by fitting Laplace probability distributions to annual dispersal distances recorded from radio-tagged sea otters (Fig. 2). Weekly locations were collected from study animals using standard VHF radio telemetric techniques (Ralls et al. 1996, Tinker et al. 2006), and annual dispersal

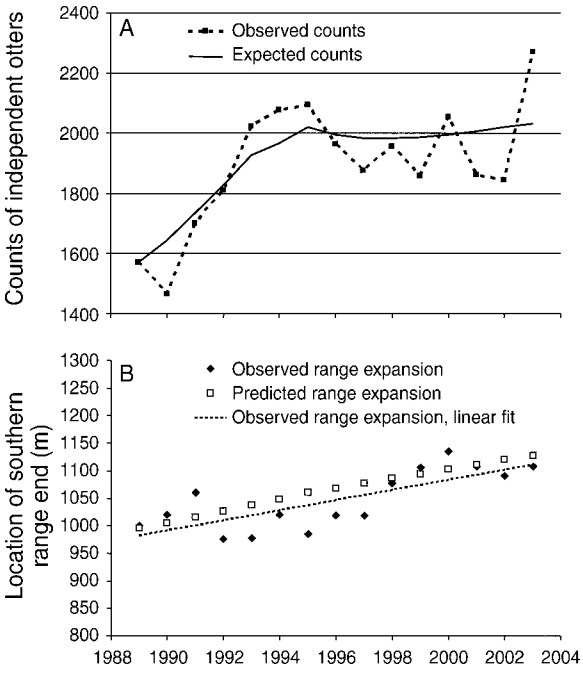

FIG. 4. Results of a hind-cast simulation of population dynamics for the southern sea otter population over the years 1989–2003. (A) Predicted population counts are plotted with actual population counts for comparison. (B) Predicted range expansion to the south is plotted with the observed range expansion for comparison: range expansion is shown as changes to the southern range end boundary (expressed as 500-m intervals along the "as-the-otter-swims" or ATOS line: see *Model development: Calculating dispersal rates* for further explanation) as a function of time. A linear, least-squares curve was fit to the observed data (dotted line) to highlight the close correspondence between the predicted and observed mean rate of southward range expansion.

distances were calculated as net linear displacement between an animal's location at week 0 and week 52 (distances were measured in kilometers along the ATOS line, where 1 km = 2 ATOS units). As with demographic rates, data were available from two time periods: the mid-1980s (Siniff and Ralls 1991) and 2001–2004 (Tinker et al. 2006). In order to obtain unbiased estimates of dispersal parameters while at the same time quantifying parameter uncertainty, a resampling approach was used for analysis: 10 animals were selected randomly (with replacement) from the total sample of animals available for a given age/sex group, study period, and region, the start date (week 0) was randomly selected, and net annual displacement was calculated based on the animal's location 52 weeks later. This process was repeated for 10 000 iterations, and then we used maximum-likelihood methods to fit Laplace probability distributions for four age/sex classes (N = 17 juvenile/subadult females, 45 adult females, 12 juvenile/subadult males, and 35 adult males). The juvenile/subadult age classes and adult/aged-adult age classes were pooled because there were insufficient sample sizes (particularly for juveniles) to allow calculation of separate distributions, but also because previous work suggested that this was an appropriate classification scheme for movement (Ralls et al. 1996). Sample size constraints precluded separate analyses for all three regions: in the case of the 1980s sample we pooled data from all areas, while for the latter sample there were sufficient data available to conduct two analyses, one for animals north of Point Sur (the northern region) and a second for animals south of Point Sur (the central and southern regions; Fig. 1). For each age/sex class, study period, and region we calculated the maximum-likelihood estimate of the Laplace parameter, $\sigma_{i,x}$, and the standard error associated with this estimate (Table 3) and used these values to parameterize movement matrices and dispersal kernel functions in model simulations.

Simulation Methods

Although it would have been possible to initialize the population vector using the stable stage distribution (SSD) associated with a particular demographic schedule (Caswell 2001), there was evidence for recent changes to the survival schedule of southern sea otters that would have precluded convergence on the SSD (Estes et al. 2003, Tinker et al. 2006). Consequently, prior to running forward simulations we ran an historical simulation in order to generate appropriate present-day stage structures for each region. We initialized 1989 population vectors for each region by multiplying the 1989 spring census counts by the SSD associated with the demographic rates of the 1980s (Table 2), which we assumed were approximately constant through to the early 1990s (Estes et al. 2003). We then projected 15 years of population dynamics (Fig. 4), calculating all demographic transitions, dispersal, and range expansion rates as explained in *Model development*, above. Specifically, we used the estimates for $\sigma_{i,x}$ calculated from the 2001–2004 data set (Table 3), and we adjusted vital rates for the fourth through 15th years of the projection (1992–2003) to equal the appropriate maximum-likelihood estimates (Table 2). The result of this historical projection was an expected population vector for 2004, which was used to initialize all forward simulations. This exercise also provided the opportunity to compare expected vs. observed population counts and expected vs. observed range expansion, thereby allowing us to graphically examine the performance of our model structure and parameter values.

After initializing the population vector we conducted 75 000 forward simulations, each using a different combination of stage- and location-specific demographic rates and dispersal parameters. We first created 500 unique sets of dispersal kernels from randomly generated Laplace distribution scale parameters: in particular, 500 random values of $\sigma_{i,x}$ were generated such that the overall mean and standard error for a given age/sex class and region corresponded to that shown in Table 3 (1980s estimates and 2001–2004 estimates were repre-

TABLE 3. Maximum-likelihood estimates of the Laplace distribution parameter, σ (in kilometers), used to parameterize dispersal kernels for the simulation model.

Region, study period	Females		Males	
	Juveniles and subadults	Adults	Juveniles and subadults	Adults
Whole range, 1984–1986	17.54 (3.53)	5.33 (0.73)	37.82 (4.41)	9.1 (1.66)
North of range, 2001–2004	10.52 (3.16)	4.82 (0.5)	91.53 (15.24)	7.27 (2.11)
South/center of range, 2001–2004	16.48 (3.36)	6.13 (1.8)	47.76 (10.37)	25.41 (7.11)

Notes: Estimates of σ represent an animal's expected dispersal distance northward along the coast, given that it moves to the north, or its expected dispersal distance southward, given that it moves south, assuming equal probability of northward or southward movement. Numbers in parentheses are standard errors associated with the maximum-likelihood estimates.

sented equally). For each of the resulting 500 movement matrices we created 150 randomly generated demographic schedules with each of the three sets of demographic estimates represented equally (Table 2). For each of the 75 000 resulting parameter sets, population dynamics and interregional movements were projected for 25 years into the future (Hunter and Caswell 2005) in conjunction with solution of the integro-difference equations to calculate annual range expansion. We defined the initial southern and northern range boundaries as the two points on the ATOS line spanning 99.5% of the spring survey count (North = ATOS 100, south = ATOS 1160, based on 2003–2004 survey data), recognizing that this designation is somewhat arbitrary and that a few individual animals will occasionally be observed well beyond these boundaries.

We summarized simulation results by tabulating three statistics: the predicted rate of range expansion to the south (in units of kilometers per year), the predicted number of independent otters south of Point Conception at the end of each simulation, and predicted growth of the population as a whole (presented as λ, the mean annual rate of growth calculated from simulation results, which we distinguish from the theoretical asymptotic growth rate derived algebraically from the projection matrix). We report the mean, median, mode, and variance for these three statistics, as well as their 95% confidence limits. We then conducted perturbation analysis (Caswell 2001) to determine the relative importance of model parameter values (specifically, the location- and stage-specific vital rates and dispersal parameters) for each model prediction. In matrix models, the potential contribution of a parameter to variation in some demographic statistic can be expressed as an analytically derived sensitivity value or an elasticity value (Caswell 2001), the latter being a measure of proportional sensitivity to proportional perturbations in a given parameter. Accordingly, for each unique parameterization of multistate matrix **B** we calculated elasticities for asymptotic population growth rate (following Caswell 2001) and asymptotic wave speed (following Neubert and Caswell 2000) with respect to vital rates and dispersal parameters; we report mean elasticity values averaged across all iterations. Next, recognizing that the potential contribution of model parameters to variation in demographic statistics may differ somewhat from the realized contribution to observed variance (e.g., Crooks et al. 1998), we performed a retrospective perturbation analysis, or "life stage simulation analysis" (LSS; Wisdom et al. 2000). Specifically, we estimated the proportion of variation in the three simulation response variables, the rate of southward range expansion, rangewide population growth, and population growth south of Point Conception, explained by each of the location- and stage-specific demographic and dispersal parameters. We used a general linear model to analyze variation of each response variable as a function of all model parameters and estimated variance components by calculating partial coefficients of determination (r_p^2), following Neter et al. (1990). Both elasticity analysis and LSS analysis can be informative, although they often provide quite different insights into model dynamics and conservation implications (Wisdom et al. 2000, Caswell 2001). We summarize both sets of results for the population as a whole and separately for each region. All results are reported along with standard errors and 95% confidence limits.

RESULTS

The historical projection simulation resulted in population dynamics that were consistent with observed survey counts over the same period and illustrate the variability in potential growth rates (reflected as changes in the slope of the "expected counts" trend line in Fig. 4A) that were possible under the simulation parameters. There was also close agreement between actual southward range expansion over the past 15 years and the predicted population wave speed. Although the position of the southern range boundary from year to year was highly variable, the long-term trend was well fit by a linear expansion rate of ~4.61 km/yr ($R^2 = 0.59$). This average realized rate was very close to our mean predicted rate of expansion over the same period (4.73 km/yr; Fig. 4B), as calculated by solving integro-difference equations that were based on demographic and dispersal data entirely independent from the range limit data.

The mean predicted rangewide annual rate of population increase (λ) across all forward simulations was 1.03 (see Table 4 for a complete list of simulation

TABLE 4. Summary of results from simulations.

Variable	Mean	SE	Median	Mode	95% CL
Annual rate of rangewide population increase (λ)	1.031	0.0203	1.037	1.037	0.996, 1.066
No. independents south of Point Conception after 10 years	112	15	112	107	69, 163
No. independents south of Point Conception after 25 years	395	78	382	332	148, 761
Rate of range expansion to the south (km/yr)	5.22	1.012	5.17	4.95	3.33, 7.11
Location of the southern range boundary after 10 years (ATOS)	1264		1263	1259	1227, 1302
Location of the southern range boundary after 25 years (ATOS)	1317		1315	1308	1260, 1373

Notes: For each variable we show the mean value from all simulations, the standard error of the mean, the median and mode (most frequently observed value), and the lower and upper 95% confidence limits for the mean, as based on simulation results. Note that the last two variables specify the geographic location along the California coast designating the southernmost end of the sea otter range at 10 and 25 years into the future, measured in "ATOS" units (500-m intervals along the "as-the-otter-swims" line; see *Model development: Calculating dispersal rates* for further explanation).

summary statistics). The rate of population increase to the south of Point Conception surpassed that of the rest of the population in almost all instances, with 95% of the simulations resulting in an annual growth rate in this southernmost population segment of 4–20%. The elevated rate of increase to the south was partly attributable to a high intrinsic rate of growth, but also reflected dispersal from other portions of the population. This interaction between dispersal and local demography resulted in continued range expansion to the south in virtually all simulations: the median predicted wave speed was 5.2 km/yr over the 25-year projection. This rate of southward range expansion would mean that after 10 years the range boundary will have moved to the proximity of Santa Barbara and after 25 years to a location just south of Carpinteria (Fig. 1), although there was a great deal of variation around these mean estimates (Table 4).

The predicted rate of range expansion was sensitive to both dispersal and survival rates, although the estimated importance of these two sets of parameters differed between the analytical elasticity analysis and the retrospective LSS analysis (Fig. 5). Elasticity analysis indicated that changes in survival rates would have the greatest potential effect on asymptotic wave speed, while the LSS analysis showed that variation in dispersal rates contributed most to variance in model predictions of southward rate of range expansion. In spite of this difference, the two analyses were consistent with respect to the relative rankings of different age classes: variation in adult female survival contributed more to variance in range expansion than survival of older or younger animals, while the dispersal of female juveniles and subadults had more impact on model predictions than dispersal of adult females (Fig. 5).

Rangewide population growth (λ) was far more sensitive to survival rates than to dispersal parameters: this was true both for the elasticity analysis (Table 5) and the LSS analysis (Fig. 6A). As was the case with wave speed elasticities, adult female survival had the greatest potential effect on λ, and this age-specific pattern also applied to reproduction parameters (although survival contributed far more to variance in λ than reproduction; Table 5). Both the elasticity analysis

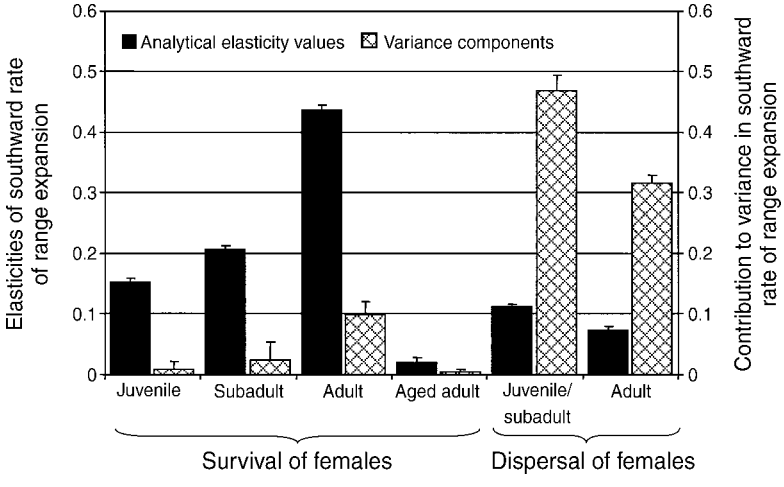

FIG. 5. Results of two perturbation analyses conducted to measure the sensitivity of the rate of southward range expansion to variation in model parameters (means + SE). Analytical elasticity values (solid bars) indicate the proportional variation in wave speed that will occur in response to proportional perturbations in age-specific movement and dispersal parameters, while variance components (hatched bars) indicate the relative proportion of variance in simulation results attributable to variation in each parameter, based on life stage simulation (LSS) analysis. Data are for female sea otters, by age.

TABLE 5. Elasticity of rangewide population growth to perturbations in age-specific and location-specific demographic rates and dispersal parameters.

Parameter	Portion of range			Total (rangewide)
	North	Central	South	
Reproduction				
Subadult	0.0074	0.0124	0.0071	0.0269
Prime-age adult	0.0276	0.0463	0.0263	0.1003
Aged adult	0.0062	0.0102	0.0058	0.0222
Subtotal	0.0411	0.0690	0.0392	0.1494
Survival				
Juvenile	0.0405	0.0709	0.0401	0.1515
Subadult	0.0783	0.1364	0.0779	0.2925
Adult	0.1469	0.2417	0.1368	0.5254
Aged adult	0.0190	0.0317	0.0183	0.0690
Subtotal	0.2442	0.4098	0.2330	0.8870
Dispersal				
Juvenile/subadult	0.0014	−0.0010	−0.0017	0.0041
Adult	0.0005	−0.0004	−0.0019	0.0028
Subtotal	0.0019	−0.0014	−0.0036	0.0069

and LSS analysis indicated that survival of animals in the central region had the greatest effect on rangewide population growth, while survival of animals in the northern and especially in the southern regions contributed less to variance in λ (Fig. 6A). Not surprisingly, this spatial pattern of survival sensitivities was reversed when we considered only population growth south of Point Conception (the southern frontal zone): survival of animals in the southern region contributed far more to the realized variance in this statistic than survival in the center or north of the range (Fig. 6B). Even more striking was the increase in the relative importance of dispersal: variation in dispersal parameters in the southern and central regions contributed most of the variance in the predicted number of animals south of Point Conception after 25 years (Fig. 6B). Female dispersal had greater effects on the rate of population increase south of Point Conception than did male dispersal (summed variance components for females = 0.497, summed variance components for males = 0.156), despite the fact that males typically exhibit greater annual dispersal distances than females and that most of the animals south of Point Conception at the present time are males.

DISCUSSION

As programs to reintroduce, or simply reduce the persecution of, wide-ranging species occur, the ability to accurately understand and predict population growth and range expansion becomes a critical management need. The predictions of our hind-cast model closely matched the historical data on rates of southward range expansion, supporting previous assertions (Lubina and Levin 1988, Krkošek et al. 2007) that estimation of asymptotic wave speed can be a useful technique for predicting range expansion of sea otters. As we show, these models can also give insight into how movement behaviors and demographic rates interact to control range expansions. Such analyses are most valuable for managers, as they allow predictions of the factors limiting recovery and also the key research and monitoring needs for reaching better predictions of recovery rate and pattern. By incorporating structured matrix methods, which are now standard for many demographic analyses (Caswell 2001, Morris and Doak 2002), into models of range expansion, we have been able to make the outputs of this modeling method far more useful for management of this population.

While it is particularly easy to apply demographic spread models to a population that is expanding relatively smoothly along a one-dimensional axis, similar approaches have been used successfully to predict invasion speed in two dimensions and in fluctuating environments (Neubert et al. 2000, Weinberger 2002, Neubert and Parker 2004). Because it can incorporate information on stage-specific and location-specific dispersal probabilities, vital rates, and population structure, the integro-difference model we present here also provides flexibility to explore the effects of regional variation and investigate the role of specific life-history processes in driving range expansion. Simple diffusion models (e.g., that were used to model invasion

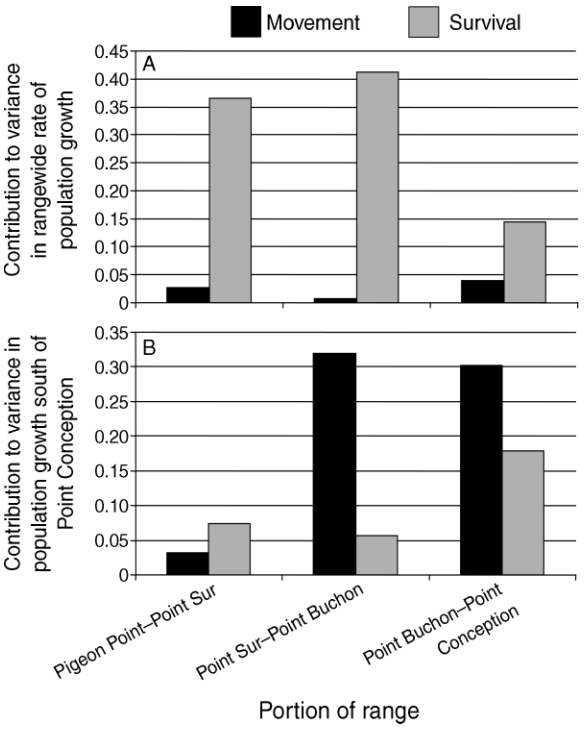

FIG. 6. Results of a perturbation, or life stage simulation (LSS) analysis, showing the relative proportion of the variance in simulation results (measured as partial coefficients of determination, r_p^2) explained by variation in movement parameters and survival parameters in different portions of the range. (A) Contribution to variance in rangewide population growth. (B) Contribution to variance in population growth south of Point Conception, California, USA.

speed in sea otters by Lubina and Levin [1988]) are conceptually simpler and require fewer data for parameterization, but they lack the ability to tie individual performance (often the target of conservation management) to population-level behavior. Although simplicity is clearly a desirable trait in any modeling exercise, the greater model complexity we employ is necessary for generating predictions of transient dynamics at regional scales, and the existence of reliable data on spatial structure with respect to density, stage-specific vital rates, and dispersal distance makes it possible to parameterize these more complex models. One key advantage of the explicit consideration of parameter uncertainty that we include in our analysis is also that it allows us to gauge whether our more detailed model is hopelessly compromised by uncertain parameter values. Reassuringly, the consistency of our results shows that this is not the case (Table 4).

Explicit analysis of uncertainty can also provide useful insights to managers (Doak and Mills 1994, Pascual and Adkison 1994). One way to incorporate uncertainty into management decisions is to consider, as in our analysis, the full range of outcomes predicted by the range of uncertainly estimated input parameters (Table 4). Using the variation in outcomes of these models, LSS analysis provides an effective tool for identifying the life-history stages and subsets of the population that contribute most to variation in model forecasts. Obtaining better estimates of those specific parameters (or better understanding of the processes that affect those parameters) will most benefit the precision and accuracy of the model predictions. For example, LSS analysis identified dispersal of juvenile and subadult females at the south end of the range as the parameter contributing most to uncertainty in predictions of southward range expansion and population growth to the south of Point Conception (Figs. 5 and 6). The discrepancy between this result and the elasticity analysis results stems from the relatively large variances associated with the dispersal parameters (Table 3). These variance estimates include both process error and sampling error components, which we could, ideally, decompose. While the limitations of our data sources led us to simply leave these grouped, we believe that most of the combined variance reflects sampling uncertainty, which could be reduced by increased sample sizes. Hence, fieldwork designed to improve estimates of juvenile and subadult female dispersal in the south of the range would do most to improve accuracy and reduce uncertainty in predicting future range expansion and the associated economic implications for tourism and fisheries industries (USFWS 2005).

A second function of sensitivity analysis is the identification of key life-history stages to target for further study or management action, with the goal of having the greatest efficacy for recovery or some other explicit objective. This is a point worth emphasizing, because these results are often not intuitively obvious. For example, although males are more likely to move longer distances than females and most of the individuals that currently travel south of Point Conception are males, female dispersal and survival was far more important in determining range expansion rates and future population growth south of Point Conception. This is not so surprising considering that range expansion by males alone would provide no intrinsic population growth (i.e., reproduction) at the ends of the range. Less intuitively, while subadult female dispersal affects range expansion more than does adult female dispersal, elasticity analysis indicated that it is actually the survival of adult females that can have the greatest potential impact on both range expansion rates and population growth (Fig. 5, Table 5), underscoring our need for a better understanding of the ultimate processes affecting adult female survival (Estes et al. 2003, Gerber et al. 2004, Tinker et al. 2006).

In spite of the range of complications that it includes, our multistate matrix model does not explicitly account for some features of population ecology likely to be important for sea otters and many other species to which this approach could be applied. These include density dependence (Laidre et al. 2001), spatial and temporal variation in habitat quality (Thomas and Kunin 1999, Virgl and Messier 2000), seasonal reproductive peaks and movement patterns (Jameson 1989), and important behavioral characteristics such as age- or sex-based segregation at smaller spatial scales (Jameson 1989). The most critical of these factors, such as density dependence and habitat quality, are implicitly present in our model, since these effects have determined past and present vital rates, distributions, and movement probabilities within different regions of the existing range (Tinker et al. 2006). Nonetheless, certain features of range expansion in sea otters such as periodic or "pulse-like" advances in range edges (Riedman and Estes 1990) are not predicted by our model. These trends may be related to temporal or spatial variation in habitat quality and prey abundance (Lubina and Levin 1988): for example, the apparent "jump" that occurred around 1998 (Fig. 4B) likely corresponds to the first large-scale movement of sea otters around Point Conception, a significant biogeographic barrier (Fig. 1) that may have discouraged earlier and more gradual range expansion. Such environmental heterogeneity can be explicitly incorporated into future models through variations to our approach (e.g., Neubert et al. 2000, Weinberger 2002).

Overall, our analysis shows how movement and demography data can be integrated to provide robust analyses of population growth and spread that can better inform policy and management decisions. This same synthesis of a multistate dispersal matrix and the integro-difference equation for estimating population growth and range expansion could be applied to other wide-ranging species, providing a useful and flexible tool for conservation biologists that can be easily modified as additional data and more precise parameter estimates

become available, as they will with rapid improvements in remote-tracking technologies. Analyses that emphasize uncertainty and the effects of different aspects of individual performance for population growth and spatial spread can dramatically increase the utility of these models for conservation management. The approach provides both guidance for the acquisition of these data and a means of forecasting the consequence of specific management actions. Our results demonstrate that this powerful analytical tool, which has been increasingly used in the study of invasive species, can also aid in the management of threatened but recovering wildlife populations as they recolonize former habitat.

Acknowledgments

We are grateful to J. Bodkin, L. Carswell, H. Caswell, A. Kage, K. Laidre, K. Ralls, and G. Sanders for their advice and contributions to the development of this model. An earlier version of this manuscript also benefited from comments and suggestions by Claudio Campagna and three other anonymous reviewers. We thank the dozens of researchers and volunteers who contributed to collection of radio telemetry data: in particular, C. Alfano, G. Bentall, B. Cummings, J. Hill, A. Kage, C. Lin, T. Nicholson, K. Sanchez, M. Staedler, J. Stewart, and B. Van Wagenen. Primary support for data collection activities was provided by a grant from the Minerals Management Service (MMS Cooperative Agreement 14-35-0001-31063) and by funding from the U.S. Geological Survey (Western Ecological Research Center and Alaska Science Center), California Department of Fish and Game, and the Monterey Bay Aquarium. Additional support for analysis was provided by a grant from "Friends of the Sea Otter" and NSF DEB-0087078 and USDA 2002-00610 to D. F. Doak.

Literature Cited

Andow, D. A., P. M. Kareiva, S. A. Levin, and A. Okubo. 1990. Spread of invading organisms. Landscape Ecology 4: 177–188.

Bales, S. L., E. C. Hellgren, D. M. Leslie, and J. Hemphill. 2005. Dynamics of a recolonizing population of black bears in the Ouachita Mountains of Oklahoma. Wildlife Society Bulletin 33:1342–1351.

Beissinger, S. R., and D. R. McCullough. 2002. Population viability analysis. University of Chicago Press, Chicago, Illinois, USA.

Berger, J., P. B. Stacey, L. Bellis, and M. P. Johnson. 2001. A mammalian predator–prey imbalance: grizzly bear and wolf extinction affect avian neotropical migrants. Ecological Applications 11:947–960.

Buckley, Y. M., E. Brockerhoff, L. Langer, N. Ledgard, H. North, and M. Rees. 2005. Slowing down a pine invasion despite uncertainty in demography and dispersal. Journal of Applied Ecology 42:1020–1030.

Caswell, H. 2001. Matrix population models: construction, analysis, and interpretation. Second edition. Sinauer, Sunderland, Massachusetts, USA.

Comiskey, E. J., O. L. Bass, L. J. Gross, R. T. McBride, and R. Salinas. 2002. Panthers and forests in South Florida: an ecological perspective. Conservation Ecology 6:18. ⟨http://www.ecologyandsociety.org/vol6/iss1/art18/⟩

Crooks, K. R., M. A. Sanjayan, and D. F. Doak. 1998. New insights on cheetah conservation through demographic modeling. Conservation Biology 12:889–895.

Crouse, D. T., L. B. Crowder, and H. Caswell. 1987. A stage-based population model for loggerhead sea turtles and implications for conservation. Ecology 68:1412–1423.

Doak, D. F., and L. S. Mills. 1994. A useful role for theory in conservation. Ecology 75:615–626.

Estes, J. A. 1990. Growth and equilibrium in sea otter populations. Journal of Animal Ecology 59:385–402.

Estes, J. A., B. B. Hatfield, K. Ralls, and J. Ames. 2003. Causes of mortality in California sea otters during periods of population growth and decline. Marine Mammal Science 19:198–216.

Estes, J. A., M. T. Tinker, T. M. Williams, and D. F. Doak. 1998. Killer whale predation on sea otters linking oceanic and nearshore ecosystems. Science 282:473–476.

Gerber, L. R., S. S. Heppell, F. Ballantyne, and E. Sala. 2005. The role of dispersal and demography in determining the efficacy of marine reserves. Canadian Journal of Fisheries and Aquatic Sciences 62:863–871.

Gerber, L. R., T. Tinker, D. Doak, and J. Estes. 2004. Mortality sensitivity in life-stage simulation analysis: a case study of southern sea otters. Ecological Applications 14: 1554–1565.

Hunter, C. M., and H. Caswell. 2005. The use of the vec-permutation matrix in spatial matrix population models. Ecological Modelling 188:15–21.

Hurford, A., M. Hebblewhite, and M. A. Lewis. 2006. A spatially explicit model for an Allee effect: why wolves recolonize so slowly in Greater Yellowstone. Theoretical Population Biology 70:244–254.

Jameson, R. J. 1989. Movements, home range, and territories of male sea otters off central California. Marine Mammal Science 5:159–172.

Jameson, R. J., K. W. Kenyon, A. M. Johnson, and H. M. Wight. 1982. History and status of translocated sea otter populations in North America. Wildlife Society Bulletin 10: 100–107.

Kauffman, M. J., J. F. Pollock, and B. Walton. 2004. Spatial structure, dispersal, and management of a recovering raptor population. American Naturalist 164:582–597.

Kenyon, K. W. 1969. The sea otter in the eastern Pacific Ocean. North American Fauna 68:1–352.

Kojola, I., J. Aspi, A. Hakala, S. Heikkinen, C. Ilmoni, and S. Ronkainen. 2006. Dispersal in an expanding wolf population in Finland. Journal of Mammalogy 87:281–286.

Kojola, I., and S. Heikkinen. 2006. The structure of the expanded brown bear population at the edge of the Finnish range. Annales Zoologici Fennici 43:258–262.

Kot, M., M. A. Lewis, and P. van den Driessche. 1996. Dispersal data and the spread of invading organisms. Ecology 77:2027–2042.

Krkošek, M., J. S. Lauzon-Guay, and M. A. Lewis. 2007. Relating dispersal and range expansion of California sea otters. Theoretical Population Biology 71:401–407.

Laidre, K. L., R. J. Jameson, and D. P. DeMaster. 2001. An estimation of carrying capacity for sea otters along the California coast. Marine Mammal Science 17:294–309.

Lensink, R. 1997. Range expansion of raptors in Britain and The Netherlands since the 1960s: testing an individual-based diffusion model. Journal of Animal Ecology 66:811–826.

Lindsey, P., J. T. du Toit, and M. G. L. Mills. 2004. The distribution and population status of African wild dogs (*Lycaon pictus*) outside protected areas in South Africa. South African Journal of Wildlife Research 34:143–151.

Lubina, J. A., and S. A. Levin. 1988. The spread of a reinvading species: range expansion in the California sea otter. American Naturalist 131:526–543.

Moro, D. 2003. Translocation of captive-bred dibblers *Parantechinus apicalis* (Marsupialia : Dasyuridae) to Escape Island, Western Australia. Biological Conservation 111:305–315.

Morris, W. F., and D. F. Doak. 2002. Quantitative conservation biology: theory and practice of population viability analysis. Sinauer, Sunderland, Massachusetts, USA.

Neflemann, C., O. G. Stoen, J. Kindberg, J. E. Swenson, I. Vistnes, G. Ericsson, J. Katajisto, B. P. Kaltenborn, J. Martin, and A. Ordiz. 2007. Terrain use by an expanding

brown bear population in relation to age, recreational resorts and human settlements. Biological Conservation 138:157–165.
Neter, J., W. Wasserman, and M. H. Kutner. 1990. Applied linear statistical models: regression, analysis of variance, and experimental designs. Third edition. Irwin, Chicago, Illinois, USA.
Neubert, M. G., and H. Caswell. 2000. Demography and dispersal: calculation and sensitivity analysis of invasion speed for structured populations. Ecology 81:1613–1628.
Neubert, M. G., M. Kot, and M. A. Lewis. 2000. Invasion speeds in fluctuating environments. Proceedings of the Royal Society B 267:1603–1610.
Neubert, M. G., and I. M. Parker. 2004. Projecting rates of spread for invasive species. Risk Analysis 24:817–831.
Pace, M. L., J. J. Cole, S. R. Carpenter, and J. F. Kitchell. 1999. Trophic cascades revealed in diverse ecosystems. Trends in Ecology and Evolution 14:483–488.
Paine, R. T. 1966. Food web complexity and species diversity. American Naturalist 100:65–75.
Paine, R. T. 1969. A note on trophic complexity and community stability. American Naturalist 103:91–93.
Pascual, M. A., and M. D. Adkison. 1994. The decline of the Steller sea lion in the Northeast Pacific: Demography, harvest or environment? Ecological Applications 4:393–403.
Pattison, C. A., M. D. Harris, and F. E. Wendell. 1997. Sea otter, *Enhydra lutris*, mortalities in California, 1968 through 1993. Administrative Report 97-5. Marine Resources Branch, California Fish and Game, Morro Bay, California, USA.
Power, M. E., D. Tilman, J. A. Estes, B. A. Menge, W. J. Bond, L. S. Mills, G. Daily, J. C. Castilla, J. Lubchenco, and R. T. Paine. 1996. Challenges in the quest for keystones: identifying keystone species is difficult—but essential to understanding how loss of species will affect ecosystems. BioScience 46:609–620.
Ralls, K., T. C. Eagle, and D. B. Siniff. 1996. Movement and spatial use patterns of California sea otters. Canadian Journal of Zoology 74:1841–1849.
Ray, J. C., K. H. Redford, R. S. Steneck, and J. Berger. 2005. Large carnivores and the conservation of biodiversity. Island Press, Washington, D.C., USA.
Riedman, M. L., and J. A. Estes. 1990. The sea otter, *Enhydra lutris*: behavior, ecology and natural history. U.S. Fish and Wildlife Service Biological Report 90:I–III,1–126.
Ripple, W. J., and R. L. Beschta. 2007. Restoring Yellowstone's aspen with wolves. Biological Conservation 138:514–519.
Shigesada, N., K. Kawasaki, and Y. Takeda. 1995. Modeling stratified diffusion in biological invasions. American Naturalist 146:229–251.
Siniff, D. B., and K. Ralls. 1991. Reproduction, survival and tag loss in California sea otters. Marine Mammal Science 7: 211–229.
Skellam, J. G. 1951. Random dispersal in theoretical populations. Biometrika 38:196–218.
Soulé, M. E., J. A. Estes, J. Berger, and C. Martinez del Rio. 2003. Ecological effectiveness: conservation goals for interactive species. Conservation Biology 17:1238–1250.
Swenson, R. O. 1999. The ecology, behavior, and conservation of the tidewater goby, *Eucyclogobius newberryi*. Environmental Biology of Fishes 55:99–114.
Terborgh, J., L. Lopez, P. Nunez V, M. Rao, G. Shahabuddin, G. Orihuela, M. Riveros, R. Ascanio, G. H. Adler, T. D. Lambert, and L. Balbas. 2001. Ecological meltdown in predator-free forest fragments. Science 294:1923–1926.
Thomas, C. D., and W. E. Kunin. 1999. The spatial structure of populations. Journal of Animal Ecology 68:647–657.
Tinker, M. T., D. F. Doak, J. A. Estes, B. B. Hatfield, M. M. Staedler, and J. L. Bodkin. 2006. Incorporating diverse data and realistic complexity into demographic estimation procedures for sea otters. Ecological Applications 16:2293–2312.
Turchin, P. 1998. Quantitative analysis of movement: measuring and modeling population redistribution in animals and plants. Sinauer, Sunderland, Massachusetts, USA.
USFWS. 2003. Final revised recovery plan for the southern sea otter (*Enhydra lutris nereis*). U.S. Fish and Wildlife Service, Portland, Oregon, USA.
USFWS. 2005. Draft supplemental impact statement—translocation of southern sea otters. U.S. Fish and Wildlife Service, Ventura, California, USA.
Virgl, J. A., and F. Messier. 2000. Assessment of source–sink theory for predicting demographic rates among habitats that exhibit temporal changes in quality. Canadian Journal of Zoology 78:1483–1493.
Weinberger, H. F. 1982. Long-time behavior of a class of biological models. Siam Journal on Mathematical Analysis 13:353–396.
Weinberger, H. F. 2002. On spreading speeds and traveling waves for growth and migration models in a periodic habitat. Journal of Mathematical Biology 45:511–548.
Wisdom, M. J., L. S. Mills, and D. F. Doak. 2000. Life stage simulation analysis: estimating vital-rate effects on population growth for conservation. Ecology 81:628–641.
Wootton, J. T., and D. A. Bell. 1992. A metapopulation model of the peregrine falcon in California: viability and management strategies. Ecological Applications 2:307–321.